

Original Article

Using Deep Learning-Based Features and Image Augmentation to Predict Brix Values of Strawberries for Quality Control

Ameetha Junaina T. K¹, R. Kumudham², Ebenezer Abishek. B³, Mohamed Shakir⁴

^{1,2}Department of ECE, VELs Institute of Science, Technology and Advanced Studies, Chennai, Tamil Nadu, India.

³Department of ECE, VelTech MultiTech Dr. Rangarajan and Dr. Sakunthala Engineering College Chennai, Tamil Nadu, India.

⁴White-box Analytics, Sydney, Australia.

²Corresponding Author : kumudham.se@velsuniv.ac.in

Received: 25 April 2023

Revised: 17 June 2023

Accepted: 13 July 2023

Published: 21 July 2023

Abstract - The fields of Computer Vision and Artificial Intelligence are rapidly developing technologies that hold promise for enhancing the economic viability of the Agriculture industry. This is an initiative to help strawberry exporters and growers to choose high-quality strawberries concerning their sweetness by automatically predicting the Brix values from their images. Using a novel dataset of 150 Strawberry images and their corresponding Brix values as labels, a deep learning algorithm called ResNet101 is utilized for feature extraction and different machine learning-based regression models are used for predicting Brix values. The image dataset is generated using a Logitech C920 HD camera, and each sample's instrumental Brix readings are collected using a Brix refractometer. Image augmentation is employed for the dataset enhancement. 70% of the entire dataset is used for training, and the remaining 30% for testing. With a high degree of Brix prediction accuracy, 96.3142%, the squared exponential GPR model is proven to be the best-fit model for this dataset. This method can significantly help provide high-quality control requirements for the strawberry sector. An RMSE value of 0.4772 and a coefficient of determination value of 0.8648 are the obtained performance evaluation metrics values during the prediction phase. Also, the MAE and MSE values obtained are 0.0233 and 0.2277, respectively. These findings show the possibility of combining deep learning with image enhancement to increase the precision of Brix value predictions for strawberries, and they may be a useful tool for enhancing the effectiveness and precision of quality control measures in the fruit business.

Keywords - Automated strawberry brix prediction, Gaussian process regression model, Image data augmentation, Machine learning and deep learning techniques, Resnet101.

1. Introduction

In recent times, there has been an upsurge in interest regarding the integration of artificial intelligence (AI) and computer vision technology into various industries, including agriculture. The utilization of image analysis is a potentially advantageous approach to forecasting the quality of fruits and vegetables. The conventional techniques employed for assessing the quality of agricultural produce are prone to errors, lack dependability, and demand substantial human effort due to the laborious nature of manual inspection. Recent developments in artificial intelligence and computer vision have enabled researchers to design automated systems capable of accurately assessing the quality of fruits and vegetables by analyzing their visual characteristics. The significance of artificial intelligence in contemporary times is evident through examining academic literature, which facilitates an understanding of the pervasive integration of machine

learning and deep learning methodologies across all aspects of human existence. Deep learning (DL) is a specialized area within the broader field of machine learning, which utilizes sophisticated algorithms to capture and represent complex, abstract concepts within datasets. The acquisition of these abstractions can be achieved through the utilization of a deep learning model without necessitating manual design. [1-2] A number of studies in the scholarly literature employ computer vision-based algorithms that utilize machine learning and deep learning methodologies to automate agricultural practices. [3-10] At its fundamental level, deep learning can be comprehended as a technique for automating predictive analytics. [11-13] Deep learning applications can be applied in various ways in today's environment. Image recognition is a widely used application. [14] The utilization of deep learning algorithms for the automated identification of image features holds significant potential for various applications within the



agricultural sector. These applications include but are not limited to harvest yield prediction, [15-17] weed identification and management, [18] harvest/plant disease identification, [19-21] harvest quality prediction and evaluation, [22-23] and irrigation optimization. [24-25] Deep learning algorithms offer several benefits over conventional methods, such as enhanced accuracy, the capacity to learn from unstructured data, the ability to extract features from data efficiently, and the capability to handle vast amounts of data. DL is having a significant impact in precision agriculture, where machine vision algorithms are used to detect and categorize various types of plants to improve crop production. The application of regression techniques based on deep learning is currently being employed within the agricultural sector. [26-27] The regression technique allows for assessing the level of correlation between a dependent variable and an independent one. In order to utilize regression methodologies, it is necessary for two variables, denoted as y and x , to exhibit a mathematical association between their respective measurements, thereby enabling the prediction of the value of y based on a measurement of the other variable, x . Through the utilization of deep learning and computer vision methodologies, researchers are able to forecast various attributes such as shelf life, quality, and optimal harvesting time based on an uploaded image. It is a huge breakthrough for farmers worldwide, who can now better understand their yield for the running year and so.

The quantification of sugar content in fruits, known as the Brix value, is a pivotal parameter in evaluating fruit quality and identifying the most suitable harvest periods. Numerous methodologies have been investigated for the purpose of predicting Brix values. However, the emergence of deep learning (DL) and its capacity to extract significant features from images has presented novel opportunities. Brix monitoring by destructive techniques includes sensory evaluation with the help of sensory panels, tools like refractometers, hydrometers, and liquid chromatography. Conventional techniques for measuring Brix entail arduous and time-consuming manual procedures, which frequently lead to imprecise measurements and delays in obtaining accurate results. [28] The precise estimation of Brix values in strawberries is of paramount importance in guaranteeing quality assurance, efficient post-harvest handling, and maximum consumer contentment. Therefore, a pressing need exists for a systematic and mechanized method to predict Brix levels in strawberries. The implementation of technology for automation enables the precise and consistent quantification of Brix values, thereby facilitating the dependable and precise evaluation of fruit quality. The implementation of quality control measures aids in the maintenance of standards and facilitates the selection of fruits with optimal sweetness levels for distribution and commercialization. Deep learning algorithms have exhibited exceptional proficiency in tasks related to image recognition, thereby presenting a viable instrument for scrutinizing the visual attributes of strawberries

and precisely forecasting their Brix values. Despite the potential of deep learning (DL) based approaches, there is a research gap in developing a simple, robust, and reliable methodology tailored for predicting Brix value in strawberries using DL-based image features.

The objective of this work is to fill the existing gap in the literature by proposing a new deep-learning framework for the prediction of Brix values in strawberries. Also, to enhance the precision and effectiveness of Brix value estimation compared to conventional techniques by utilizing the innate abilities of deep learning algorithms to acquire distinctive characteristics from strawberry images autonomously. Two distinct deep-learning techniques were employed to predict the Brix value from strawberry images. The second method was found to be superior and is expounded upon in this report. The investigation was carried out utilizing solely merged visual representations of strawberries and their corresponding Brix measurements as image labels. The datasets were utilized to train the regression model, which was subsequently employed to forecast the Brix values of the test samples. The dataset was enhanced using an image data augmentation technique, and ResNet101, a pre-trained CNN model, was used to extract image features, both of which contributed to a significant improvement in prediction accuracy (Method 2). Quality control would entail evaluating the strawberries' quality using the anticipated Brix readings. Strawberries that do not reach the required quality standard can be easily identified by precisely forecasting the Brix values. Then the necessary action can be taken to eliminate them from the production or distribution process. The implementation of this approach has the potential to improve customer satisfaction and reduce waste by guaranteeing the delivery of high-quality strawberries exclusively to end users.

2. Literature Review

2.1. Brix Prediction Algorithms in Literature: A brief review

In the research, "Forward Feature Selection for Ensembles to Predict Brix Values in Mango Fruits based on NIR Spectroscopy Technique," Bowonsak Srisungsittisunti makes use of ensemble models with forward feature selection to forecast Brix levels in mangoes using datasets from NIR spectroscopy. [29] The objective of this investigation was to construct precise forecasting models that can be utilized to approximate the Brix values of mango fruits. To achieve this goal, the investigators employed ensemble models that incorporated linear regression (LR), neural networks (NN), and k-nearest neighbor (KNN) methodologies. In addition, forward feature selection was utilized to identify the most pertinent features within datasets of near-infrared spectra. The researchers utilized spectrum data obtained through NIR spectroscopy from four distinct groups of 300 mango fruits to generate datasets for training ensemble models. A comprehensive set of 112 ensemble models were constructed, comprising different combinations of distinct methodologies and datasets. The empirical findings showed that mangoes that

underwent an extended harvesting period demonstrated reduced values of standard deviation (SD) and root mean square error (RMSE). The LR ensemble model that underwent training with the dataset of a 120-day harvesting period, and feature selection through all three methods (3M120), had been observed to exhibit the lowest RMSE value. The LR-NN-KNN ensemble model, trained using the data of a 120-day harvesting period and feature selection through the KNN method, exhibited the best performance in predicting the optimal Brix value. This was evidenced by the model's minimum standard deviation value and an RMSE value close to the minimum. This paper shows the importance of picking the right features and model combinations to get the best prediction performance by comparing the outcomes from the feature selection and prediction stages.

In a study conducted by Al-Sammarraie et al. (2022), the authors explore the potential of using AI for the problem of determining the sweetness of oranges by analyzing the correlation between sweetness and the colors red, green, and blue (RGB) values in fruit evaluations, as the latter may affect the former. [30] In this work, an orange fruit image dataset was used alongside the Orange data mining tool and many machine learning methods. The objective was to identify the algorithm that yielded the highest precision in forecasting sweetness.

The results emphasized the predominant impact of the red color constituent in forecasting the degree of fruit sweetness, indicating a direct correlation between the red color variable and the degree of sweetness. Logistic regression, tree method, SVM, neural network, and KNN were evaluated for their effectiveness in predicting sweetness. The results indicated that logistic regression achieved the highest accuracy rate of 97%, followed by the tree method at 96%, SVM at 93%, neural network at 88%, and KNN at 82%. The concluding statements suggest that color feature values have the potential to serve as reliable indicators of fruit sweetness.

3. Materials and Methods

This investigation aims to devise an automated methodology for forecasting the Brix levels of strawberries from their images. This will be accomplished by employing machine learning-driven regression models that rely exclusively on associated images as input. The study involved the collection of two distinct sets of data, specifically the strawberry image dataset and the corresponding lab (instrumental) values of ⁰Brix, which were utilized as labels for the images.

3.1. Acquisition of Dataset

MAHABALESHWAR strawberries were gathered from fresh produce marketplaces during the months when they were in season to build a dataset. Table 1 displays the details about the number of strawberry samples used for dataset acquisition over some period (Oct 2020- Feb 2021).

Table 1. Dataset collection details

Month	Oct-Nov	Dec	Jan-Feb	Total
Qty. Sampled	55	35	60	150

The task of collecting strawberry samples was challenging during the pandemic period due to the limited availability of the fruit. Moreover, obtaining both datasets (i.e., Image and Instrumental Brix value readings) necessitated additional precautions to ensure the dependability of the outcomes. A studio setup and a Logitech C920 HD camera were used to take high-quality pictures of strawberries. [31] The strawberry fruit was positioned centrally within the setting and was captured in a stationary position with respect to the camera against a white backdrop. The visual representation in Figure 1 showcases the integration of a strip of Light Emitting Diode lights within the studio configuration, with the purpose of attaining a suitably illuminated backdrop. Additionally, the refractometer utilized in the experiment is visible in the image.



Fig. 1 Studio setup for image acquisition. [31]

Figure 2 shows different strawberry perspectives. After vertically cutting the sample, a cross-section was also considered.



Fig. 2 Different views of a Strawberry sample (a) Front view 1, (b) Vertical cross-sectional view, (c) Front view 2

A precise incision was made on the strawberries using a sharp knife to obtain the instrumental Brix values. The Brix (⁰Bx) values were then determined in the laboratory by extracting the juice from each strawberry sample and measuring it with a Brix refractometer. Wine, sugar, fruit, and honey sectors all are utilizing this unit of measurement known as Brix (⁰Bx) to calculate the sugar content of products. [32]

1.0-degree Brix is equivalent to 1.0% sugar by mass in fruit juices. This generally has a positive correlation with observed sweetness. The easiest and most accurate tool for measuring Brix is a BRIX (°Bx) refractometer which measures Brix on a scale of 0 to 30 percent (% Brix), is illustrated in Figure 3(a). [33] The parts of the refractometer are displayed in Figure 3(b).

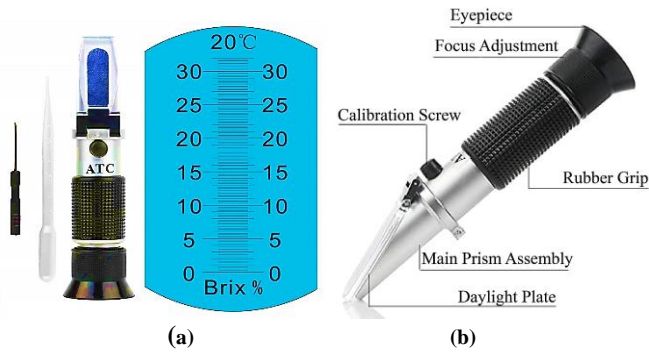


Fig. 3 BRIX Refractometer (a) Reading scale, and (b) Parts explained

The sweetness of fruit can be determined by analyzing the percentage of sugar present in the juice, which is measured in degrees Brix (°BRIX) through the assessment of its soluble solids. The instrument underwent an initial calibration process to ensure precise measurements. The experimental conditions encompassing the ambient temperature and pressure were duly recorded. The Brix values of 150 strawberry samples were recorded meticulously in a tabular format alongside their respective data samples. Table 2 presents a selection of Brix values and their corresponding sample image names, which were acquired through the employment of the Brix refractometer.

Table 2. Obtained Instrumental BRIX Dataset

Sample Name	°BRIX Values
#1.jpg	5
#2.jpg	5
#3.jpg	7.5
#4.jpg	7
#5.jpg	8.9
#6.jpg	3.9
#7.jpg	6.2
#8.jpg	5
#9.jpg	5.6
#10.jpg	7
#11.jpg	6

This methodology was easily executed by utilizing a pair of dataset values derived from a sample size of 150 strawberries. Figure 4 presents the method overview diagram of the prediction model, specifically Method 2. The below section explains in detail how this was achieved. The algorithm was implemented and executed using Matlab R2019-b Version. The activation of the parallel computing

toolbox was implemented to attain efficient execution speed. The study employed a 64-bit Microsoft Win11 operating system, an Intel(R) Core(TM) i7-9750H central processing unit clocked at 2.60GHz, 16.0 GB of random access memory, a 2T hard disk drive, and an 8G NVIDIA GeForce GTX 2080 TI graphics processing unit. Following the procurement of the dataset, the collection of 150 strawberry images stored in the system directory was imported into the Matlab workspace as a preliminary measure. The instrumental Brix values of 150 strawberries were imported into Matlab and subsequently stored in the workspace. After that, a Matlab ImageDataStore object was instantiated utilizing the aforementioned images. [34] Certain preprocessing steps were performed on the images contained within the data repository. By default, Matlab stored the image files in the natural order within the ImageDataStore. The image files were systematically organized through programming techniques to sequence the files in ascending numerical order, corresponding to their assigned sample numbers. Following the completion of natural sorting, the ImageDataStore assigned labels to each strawberry image file based on their corresponding instrumental Brix values. The dataset was enhanced through the utilization of the image data augmentation technique on the images. The utilization of image augmentation is a methodology implemented in the field of deep learning with the aim of enlarging the scope and variability of a given dataset. Consequently, the model's performance may improve as it becomes more adept at generalizing to novel and untested images. The function named 'imageDataAugmenter' produces an object for image augmentation that offers various choices for arbitrary transformations such as scaling, rotation, and X and Y reflections. The parameters can be modified based on the model's requirements and the dataset's idiosyncrasies. The variable denoting input size determines the dimensions of the images employed for training the deep learning model. All images underwent a resizing process to achieve a uniform size of 224 x 224 pixels and were in RGB color format. The function 'augmentedImageDatastore' generates an augmented ImageDataStore entity, denoted as 'imdsAugmented', that retains the dimensions of the input size. This is achieved by providing the original image datastore 'imds' and the image augmentation object 'augmenter' as inputs. The images that were initially obtained and the images that were improved through the application of the augmenter's modifications are both retained in a distinct data repository, denoted as 'imdsCombined'. The aggregate quantity of images contained within the recently created ImageDatastore is determined by summing the number of original visuals with the number of augmented ones that have been generated. This procedure facilitates the computation of the overall quantity of images contained within the resulting collection. A dataset comprising a sum of 300 images was available for regression analysis. A novel datastore was created, containing a doubled quantity of images. The initial 50% of the images corresponded to the original dataset, while the remaining 50% consisted of augmented images.

Input 1: Preprocessed Image Dataset

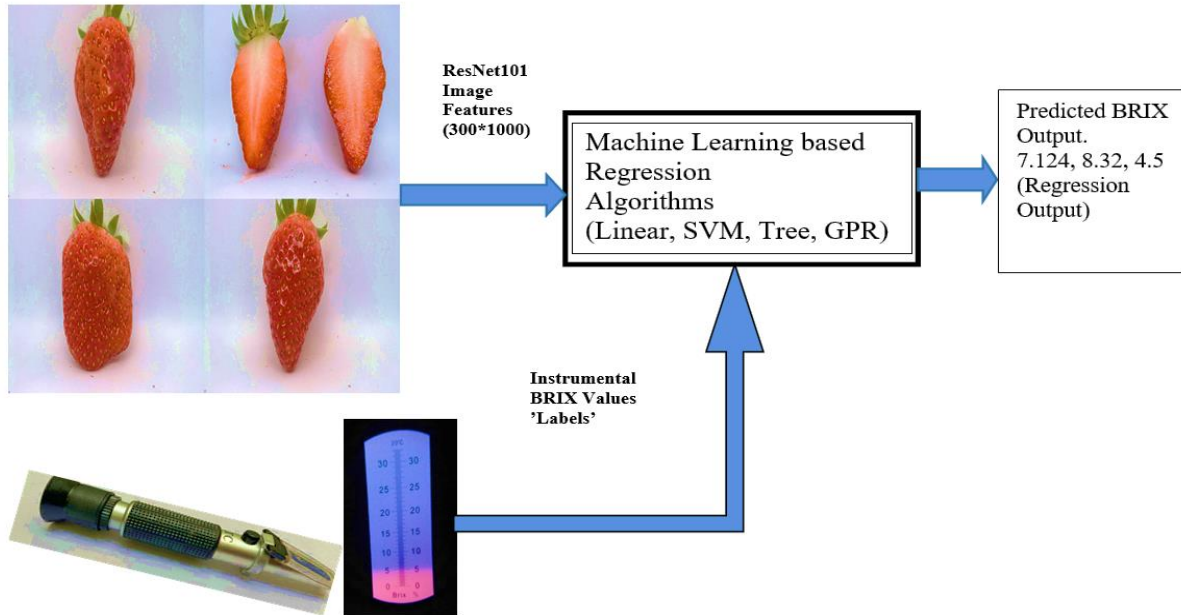


Fig. 4 Proposed method overview

A new categorical variable, 'labelsCombined', was also generated by concatenating the original labels from 'imds' with themselves. This is because the augmented images are generated from the original images and therefore have the same labels. The next step was to assign the new combined labels to the 'Labels' property of the 'imdsCombined' datastore. Thus there were a total of 300 images stored in the ImageDataStore, along with 300 corresponding labels for training and testing purposes. Pre-trained Convolutional Neural Networks were used for feature extraction from images. [35] The ResNet-101 convolutional neural network, pre-trained on the ImageNet database consisting of over one million images, is utilized for feature extraction. Consequently, the network has obtained comprehensive feature representations for diverse images. The Deep Learning Toolbox Model for the ResNet-101 Network support package needs to be downloaded and installed before using the ResNet-101 pre-trained network for feature extraction. Then the pre-trained ResNet-101 neural network model is loaded, which defines the feature layer to be used for feature extraction from the input images. The input images undergo preprocessing to align their dimensions with the input layer of ResNet-101, which is (224*224*3) using an augmented image Datastore. The activations of the feature layer were extracted for each image in the data store using the activations function. The resulting features were normalized and stored in a table with the corresponding labels as a column. These features and labels saved in the table will be used for training the regression models. ResNet-101, a deep convolutional neural network, is a popular design for detecting image features. The proposition was put forth by He et al. (2016) in their scholarly article titled "Deep Residual Learning for Image Recognition". [36] The

original ResNet architecture is expanded upon in ResNet-101, where there are 101 layers total in the ResNet-101 model, including activation functions, convolutional layers, batch normalization layers, and residual blocks. [37] The residual blocks, which constitute the primary element of the ResNet framework, facilitate the propagation of gradients in exceptionally deep networks. Furthermore, ResNet-101 employs skip connections for the purpose of connecting the input and output of each residual block, thereby mitigating the problem of vanishing gradient. Due to its high accuracy and efficiency, ResNet-101 is commonly employed as a feature extractor for transfer learning and fine-tuning other image recognition tasks. Following the extraction of features, the data pertaining to these features was organized in a tabular format, whereby the normalized features were allocated to the columns, and the corresponding labels were assigned to a distinct column. The table's dimensions were 300 by 1001, comprising 1000 image feature variables obtained from 300 images of strawberries and a single Brix label assigned to each image. Once this was done, a subset of the 300 image samples was allocated for training the network, while the remaining samples were reserved for testing. Specifically, 70% of the total sample was designated for training purposes, with the remaining 30% reserved for testing. This was accomplished using a cross-validation partition object. A training ratio of 0.7 was employed. Thus the extracted features from a total of 300 image samples of strawberries were partitioned to be utilized for the purpose of training giving 210 samples, while features from 90 image samples were reserved for testing. The 'HoldOut' technique was employed in splitting the dataset so that a random subset of the collection was used for testing while the remaining data was utilized for training. The

variable "test indices" is utilized to extract the indices of the testing subset from the cross-validation entity. The training features and labels are assigned to the Xtrain and Ytrain variables, respectively, utilizing the training indices obtained from the cross-validation object to correspondingly represent the training data and labels. The testing features and labels are assigned to the Xtest and Ytest variables, respectively, utilizing the test indices obtained from the cross-validation object. The utilization of a machine learning model can involve its training on its subsequent training set, followed by an evaluation of its performance on the resulting testing set. The holdout method is a rapid and precise technique for assessing the efficacy of a model. Figures 5 and 6 depict the histograms of the Brix values for the 210 training and 90 test data samples, respectively.

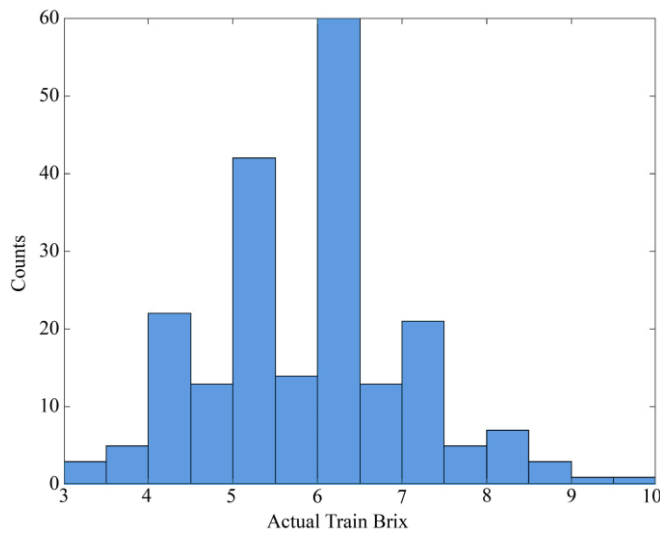


Fig. 5 Histograms of Brix values of the training dataset

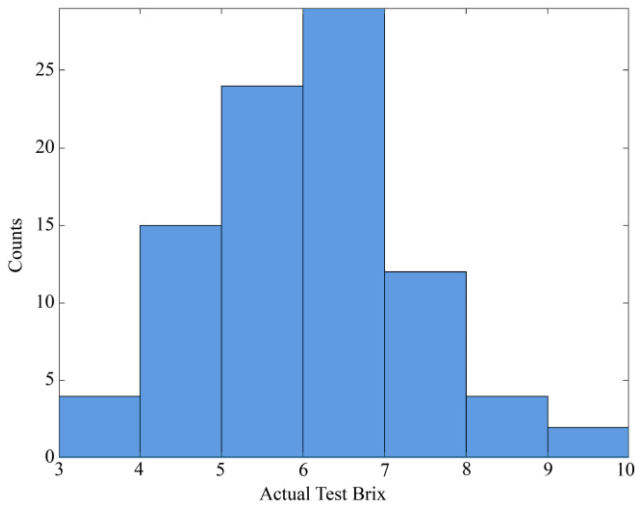


Fig. 6 Histograms of Brix values of the test dataset

The subsequent phase entails the identification of predictor and response variables for the purpose of conducting

regression analysis. The regression learner application facilitates the execution of multiple regressions in parallel. The predictor and response variables of the training samples were selected for regression, as depicted in Figure 7. It should be noted that the figure below only displays the last few features due to the difficulty in displaying the 1000 predictors of the 210 samples. Upon completion of the selection of the training dataset's predictor and response variables, the regression session was initiated, wherein multiple regression techniques, such as linear regressions, SVM regressions, Gaussian process, etc., were executed concurrently. The methodology employed involved utilizing a holdout-validation approach as selected before training. The utilization of the holdout method, particularly through the incorporation of a distinct validation set, facilitates the identification and alleviation of overfitting. The performance of the training model was evaluated using holdout validation, with a holdout size of 25%. The dataset comprised 210 training samples, with each sample containing a thousand features. In this methodology, a subset of the training data amounting to 25% (approximately 52-53 samples) was designated as a validation set, while the remaining 75% (approximately 157-158 samples) were allocated for training the model. The model underwent training using a total of 157-158 training samples, each of which was associated with thousand features. Following this, the trained model's performance was assessed on the validation set, which consisted of approximately 52 to 53 samples. The estimations generated by the trained model on the validation set were juxtaposed with the real values or labels of the validation samples, thereby offering an assessment of the model's capacity to extrapolate to unfamiliar data. It is important to acknowledge that the presence of a restricted number of validation samples may introduce a certain degree of variability in the estimated performance.

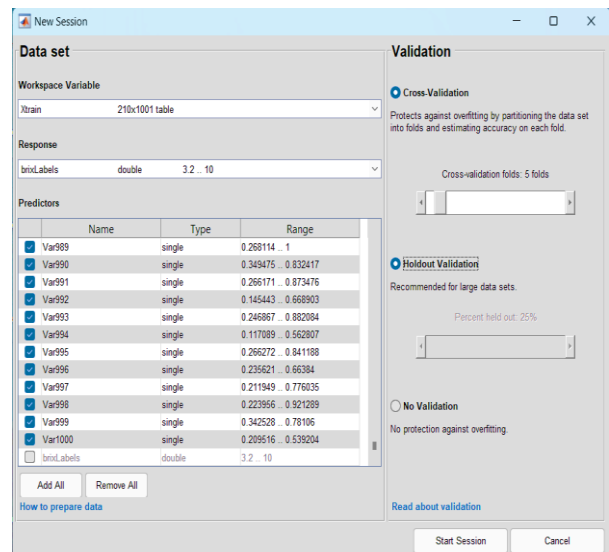


Fig. 7 Selection of predictors and response variables for ML-based regression algorithms. (Only the last few features, 989 up to 1000 feature selection, is displayed here)

Nevertheless, despite this constraint, employing holdout validation with a 25% holdout can still yield valuable insights into the model's performance and aid in making well-informed choices pertaining to model selection and hyper parameter tuning. After training, the optimal model selection was determined by the attainment of the lowest validation error metrics. The Gaussian Process Regression model, utilizing a constant basis function and Squared Exponential kernel function, has been determined to be a highly suitable model for this dataset. Following training, the model achieved a minimum RMSE value of 0.75001 and an R^2 value of 0.57. Figure 8 displays the results obtained after the training process. Multiple regression models were trained concurrently, and the model exhibiting the lowest validation errors was chosen as the optimal model. The Gaussian Process Regression Squared Exponential model has demonstrated superior suitability for the strawberry image dataset. After the completion of the training process, the obtained Mean Squared Error (MSE) value was 0.5625, while the Mean Absolute Error (MAE) value was 0.35277. The GPR model required a total training time of 3.1789 seconds for the entire training process. The bar plot in Figure 9 illustrates a comparison of the root mean square error (RMSE) values obtained from multiple training models after the training process. The GPR Squared Exponential model yielded the minimum Root Mean Square Error (RMSE) value, indicating its optimality for this dataset.

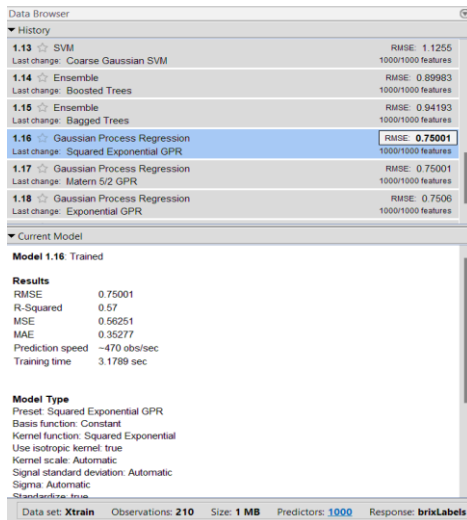


Fig. 8 Results Obtained after the training process (Squared Exponential GPR model: Optimal model)

Subsequently, this optimal model was exported to the workspace for further testing. The exported regression model is then employed to forecast the Brix values of the remaining test data samples. This was achieved by moving the remaining image features of the test data samples (90*1000) to the 'predictFcn' function in Matlab. The Brix values of the 90 samples under test were predicted with a high degree of precision. The following section elucidates the outcomes derived after forecasting the Brix values of the test data samples.

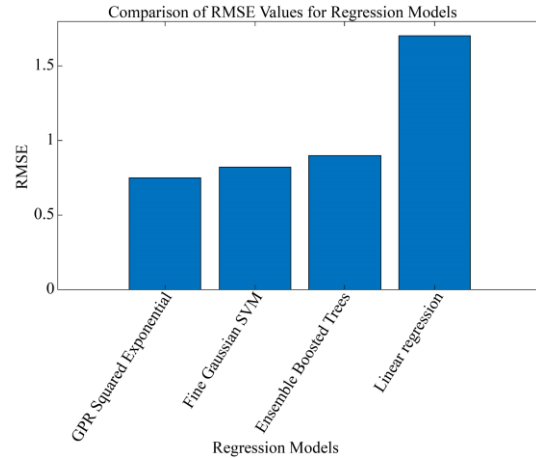


Fig. 9 Bar Plot of the RMSE Values obtained for Various Regression Models after Training

4. Results

This section provides an account of the results obtained from the training and testing protocols implemented on the dataset subsequent to conducting regression analysis. The predicted outcomes are stored within a matrix in the Matlab environment. Subsequently, a table of output is created using Matlab to exhibit the findings. Table 3 presents the strawberry names, accompanied by their respective instrumental Brix values and predicted Brix values, for a select number of samples within the test dataset. In this context, the process of identifying test strawberries is accomplished by means of their respective image names. This table facilitates the facile visual juxtaposition of the predicted Brix values with test samples' actual instrumental Brix values. Furthermore, the output figure presents the actual versus predicted Brix values of a subset of randomly selected test data samples, along with their corresponding images. Figures 10 and 11 exhibits the outcomes of the 38th and 55th samples, respectively, along with pertinent details such as sample number, instrumental Brix value, and predicted Brix values.

Table 3. Output table: Actual Vs. Predicted Brix values of a few test samples

Strawberry ID	Actual BRIX	Predicted BRIX
'2.jpg'	'5'	5.83165297067182
'4.jpg'	'7'	6.99989186111522
'6.jpg'	'3.9'	3.90017878831613
'7.jpg'	'6.2'	6.19996590684449
'9.jpg'	'5.6'	5.60002144114144
'12.jpg'	'6'	5.83165297067173
'23.jpg'	'6.9'	5.83165297063923
'32.jpg'	'7'	5.83165297067182
'33.jpg'	'6.9'	6.89990111683138
'36.jpg'	'5.9'	5.83165297525884
'41.jpg'	'3.5'	5.83165297067182
'42.jpg'	'5.2'	5.83165297067182
'45.jpg'	'6.4'	5.83165297067182
'49.jpg'	'5'	5.00007697543839

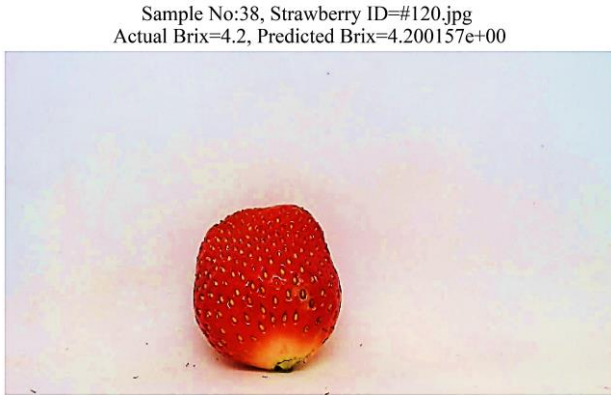


Fig. 10 Actual Vs. Predicted BRIX of 38th sample.



Fig. 11 Actual Vs. Predicted BRIX of 55th sample.

Figure 12 depicts the scatter plot of the actual versus predicted Brix values of the test data samples. The graph between actual and predicted values is depicted in Figure 13. The predicted Brix values (yfit) are contrasted with the actual Brix values (ytest) using this graph. The blue colored line represents the observed ground truth values, while the red represents the predicted values. The model's accuracy in predicting the Brix values can be assessed by contrasting the two lines. The graph shows that the model successfully predicts the Brix values as the red line overlaps the blue line at most of the graph regions as displayed.

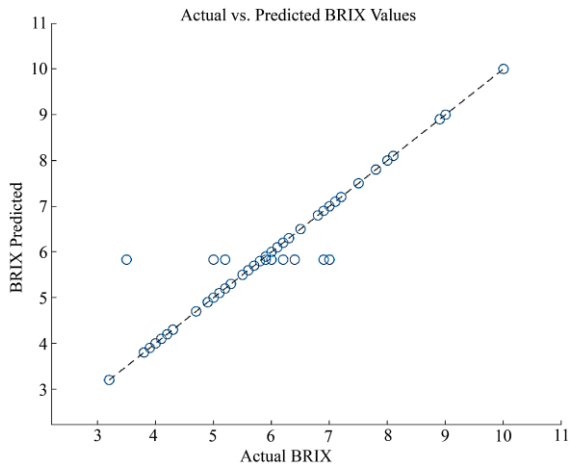


Fig. 12 Scatter plot of test data samples

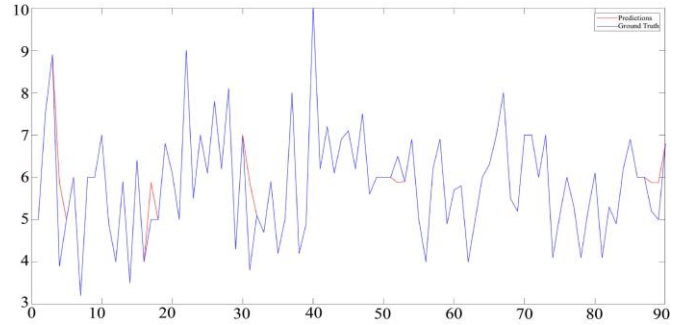


Fig. 13 Ground truth versus predictions graph

4.1. Performance Evaluation of the System

The equations listed below are used to calculate statistics metrics for the regression prediction system, such as Mean Absolute Error (MAE), Mean Squared Error (MSE), Root Mean Squared Error (RMSE), and Mean Absolute Percentage Error (MAPE), for the performance evaluation of the algorithm [38]. Using the mentioned Equation 1, MAE is calculated.

$$MAE = \left| \frac{1}{n} \sum_n (Actual\ Brix - Predicted\ Brix) \right| \quad (1)$$

Where the variable n represents the cardinality of the test dataset.

Calculating other parameters for the Brix value prediction algorithm, such as the Mean Squared Error and the Root Mean Squared Error (RMSE) of the test samples, requires using Equations 2 and 3, respectively, as shown below.

$$MSE = \frac{1}{n} \sum_n (Actual\ Brix - Predicted\ Brix)^2 \quad (2)$$

$$RMSE = \sqrt{\frac{1}{n} \sum_n (Actual\ Brix - Predicted\ Brix)^2} \quad (3)$$

The mathematical expression presented in Equation 4 is utilized to compute the coefficient of determination (R^2) metric. The metric that quantifies the degree of similarity between the data and the fitted regression line is referred to as R-squared in statistics. The term "coefficient of determination" is an alternative nomenclature for the aforementioned concept. The R-squared method is utilized to ascertain the percentage of the variance in the dependent variable that the independent variable can explain.

$$R^2 = 1 / (RSS - TSS) \quad (4)$$

where RSS = Residuals sum of squares,

TSS = Total sum of squares.

The total sum of squares is calculated by summing the squared differences between the observed values and their averages. The difference between the actual and projected

values is referred to as residuals. In order to assess how well the prediction algorithm works, the value of another metric known as the Residual Predictive Deviation (RPD) was also computed, which was done using Equation 5.

$$RPD = \frac{\sigma(A_t)}{\sigma(A_t - P_t)} \quad (5)$$

Where $\sigma(A_t)$ is the Std. Deviation of Actual Brix values(Ytest) of Test samples.
 $\sigma(A_t - P_t)$ is the Std. Deviation of Residuals.
 P_t is the predicted Brix values of test samples(Yfit).

An RPD value of 2.7 was obtained. The RPD value is obtained by dividing the std. deviation of the actual Brix values (Ytest) to the residuals' (Ytest - Yfit) std. deviation. It evaluates the prediction performance of the regression model. [39] Higher RPD values usually mean better prediction. RPD value interpretation depends on application and circumstance. However, these criteria are generally applicable: When the value of RPD falls between 1 and 1.5, it indicates a moderate level of predictive accuracy. The model exhibits a certain degree of predictive capability for the target variable, albeit with restricted precision. When the value of RPD falls between 1.5 and 2.5, it indicates a favorable level of predictive performance. The model exhibits a satisfactory level of predictive accuracy, effectively capturing a substantial proportion of the variances present in the dataset. An RPD value exceeding 2.5 signifies a substantial degree of predictive precision. This model exhibits a significant degree of precision in forecasting the dependent variable, implying robust explanatory capability.

The next step is to construct a table in order to evaluate the Mean Absolute Percentage Error. The accuracy of the prediction algorithm can be determined with the help of the MAPE. In the order given above, the table's columns list the actual instrumental Brix, the predicted Brix values, the absolute difference between the actual and predicted Brix, and the percentage difference between the original and predicted Brix. The Mean Absolute Percent Error (MAPE) is determined by averaging the fourth column of the table for all of the test data samples. This is done in order to compute the error. As a consequence of this, the MAPE value that was calculated for the prediction of 90 different test data samples came out to be 3.6858. In order to calculate MAPE, Equation 6 was utilized.

$$M = \frac{1}{n} \sum_{t=1}^n \left| \frac{A_t - P_t}{A_t} \right| \quad (6)$$

Where M is the MAPE, and n represents the variable denoting the number of iterations in the summation process.

A_t =Actual Brix Value

P_t =Predicted Brix Value

To ascertain the precision of the system, quantified as a percentage, Equation 7 directs to subtract the MAPE value from 100.

$$Accuracy(\%) = 100 - MAPE \quad (7)$$

Table 4 displays the readings from a few samples that are utilized in the computation of the MAPE. The accuracy of predicting the Brix values of the given test data samples obtained was 96.3142%. The system demonstrates an outstanding performance with regard to its accuracy percentage and other related metrics. Table 5 presents the statistical performance metrics summary obtained during both phases. The MAPE and accuracy attained in the prediction phase of Brix values are also mentioned.

An alternative approach was implemented initially to forecast the Brix values, which involved utilizing a convolutional neural network (CNN) regression technique on the same image dataset (Method 1). This method did not involve using any image data augmentation technique or pre-trained networks. A CNN-based regression technique was applied to predict the Brix values of strawberries. The predictive model demonstrated a level of accuracy of 82.6071%; after acquiring and importing images and their corresponding Brix values for 150 strawberry samples, an ImageDataStore entity was created in the Matlab environment. By default, the ImageDataStore stores the image files in their natural order. The orderly organization of image files was achieved through programming techniques to enable their arrangement in ascending numerical order according to the assigned sample numbers.

Upon the completion of the natural sorting process, the ImageDataStore allocated the appropriate instrumental Brix values to each individual strawberry image file. A set of 150 images was partitioned into two distinct subsets for the purpose of training and testing a network. Precisely, 70% of the entire sample was designated for the purpose of training, whereas the remaining 30% was set aside for testing. The training dataset comprised 107 strawberry images, whereas the testing dataset consisted of 43 images. The training and test images contained in the data repository underwent various preprocessing procedures. The datastore elements underwent an initial restructuring process, resulting in the formation of arrays that possessed four dimensions. The determination of the input layer size of the neural network as [227*227*3] was made prior to the commencement of the regression analysis. As part of the preprocessing phase, the input images underwent a resizing operation to achieve the specific size. The layers comprising the model for DL have been defined and constructed. The architectural design of the model was initially defined by its multiple layers. This prediction algorithm utilizes a custom-designed Convolutional Neural Network (CNN), which is an essential tool in the domain of Deep Learning (DL).

Table 4. Values for the computation of MAPE and Accuracy

Actual BRIX	Predicted BRIX	Absolute Difference	Absolute Percentage Error
5	5.83165297067182	0.831652970671816	16.6330594134363
7	6.99989186111522	0.000108138884777453	0.00154484121110
3.90000000000000	3.90017878831613	0.000178788316127054	0.00458431579812
6.20000000000000	6.19996590684449	3.40931555120605e-05	0.00054988960503
5.60000000000000	5.60002144114144	2.14411414374283e-05	0.00038287752566
6	5.83165297067173	0.168347029328269	2.80578382213781
6.90000000000000	5.83165297063923	1.06834702936077	15.4832902805909
7	5.83165297067182	1.16834702932818	16.6906718475455
6.90000000000000	6.89990111683138	9.88831686195013e-05	0.00143308940028
5.90000000000000	5.83165297525884	0.0683470247411568	1.15842414815520

Table 5. GPR squared exponential regression model statistical performance summary

Phase	MSE	RMSE	R ²	MAE	MAPE	ACCURACY
Training	0.56251	0.75001	0.57	0.35277	-	-
Prediction	0.2277	0.4772	0.8648	0.0233	3.6858	96.3142%

The study utilized a convolutional neural network with 24 layers to evaluate the visual information present in the images. The CNN was designed and taught with the training set to make predictions on the Brix values of the test dataset through the utilization of the implemented network. The size of the input layer, which serves as the initial layer of the neural network, was taken into account for the purpose of resizing the images. The fundamental architecture of a network is predominantly determined by its internal layers, which serve as the primary locus for computation and learning. A model's final layers determine the output data's dimensions and format. In order to facilitate the ability of a regression network to provide prognostications pertaining to uninterrupted data, such as Brix value derived from images, a fully connected regression output layer was produced upon the culmination of the procedure. In the end, the different layers were consolidated into a vertically arranged structure. The training parameters, such as maxEpochs and MiniBatchSize, were determined. The study employed a maximum of 200 Epochs and a mini-batch size of 10. The MiniBatchSize is a discrete numerical value denoting the magnitude of the mini-batch that is processed during every iteration of the training process. The variable maxEpochs represents the upper limit of epochs utilized during the training process and was defined as a positive integer. The 'rmsprop' optimization algorithm was employed as the solver.

At the onset, a learning rate of 0.001 was selected. The program's accuracy is periodically calculated after training the neural network with the training data. Throughout the training

process, it is achievable to assess the advancement of the training by generating visual depictions of diverse data points. As an illustration, it is possible to verify the rate at which the precision of the network is improving and to determine if it is exhibiting signs of overfitting the training dataset. Following each iteration, the 'trainNetwork' function generates a visual representation and presents training metrics. The network parameters are modified during each iteration, and the gradient is approximated. Upon each execution of the trainNetwork function, the system was validated by providing validation data in the trainingOptions parameter, and subsequently, the validation metrics were visually presented. The 'trainNetwork' function in Matlab was utilized for deep learning-based classification and regression tasks to train convolutional neural networks (CNNs). The process of training the network involves feeding the training images, their corresponding labels, the pre-defined network layers, and the previously established training options into the network training function. Enabling the training progress plot in the training options results in displaying the training progress figure in the plot. Upon completion, a final plot was obtained, as depicted in Figure 14. The figure depicts the root mean square error (RMSE) for regression networks instead of a plot comparing accuracy and iteration. The performance metric values obtained after training are presented in Table 6. Upon completion of the model training process, the subsequent step involves conducting testing procedures to forecast the Brix values of the test images. This entails utilizing the trained network model to evaluate the remaining test images.

The process of forecasting the Brix values of the test images were executed by feeding the taught model and the test images into the prediction function in Matlab, following the tweaking of the aforementioned network. Following the conclusion of the testing procedure, an assessment was conducted on the effectiveness of the prediction system through the utilization of several statistical metrics, including Mean Absolute Error (MAE), Mean Squared Error (MSE), Root Mean Squared Error (RMSE), Mean Absolute Percentage Error (MAPE), and Accuracy. These metrics were evaluated using the equations specified in the preceding section. MAE obtained using this approach is 0.214. MSE obtained using Equation 2. is 1.4486, and RMSE is 1.2036. The coefficient of determination yielded a value of 0.0787. The MAPE value obtained after predicting 43 test data samples using this approach is 17.3929. An accuracy of 82.6071% was obtained for this particular prediction algorithm which is pretty much only a fair accuracy. The performance metrics obtained from the utilization of both methods (methods 1 and 2) are juxtaposed and evaluated through the graphical representation depicted in Figure 15. The performance metrics, including Mean Absolute Error (MAE), Mean Squared Error (MSE), Root Mean Squared Error (RMSE), and R-squared (R^2) values, for both methods are presented in the bottom bar plot. Additionally, the accuracy achieved by both methods is compared in the top

graph (indicated by the color red), revealing that method 2 outperforms method 1.

5. Discussion

This research introduces a simple and innovative method for predicting Brix values in strawberries. The subsequent passages highlight the originality of the suggested algorithm and draw comparisons with prior research findings. The novelty of this research is attributed to the fusion of machine learning and deep learning methodologies with image features that have been extracted from a dataset comprising 300 images of strawberries. The dataset comprises 300 images, half of which were obtained via a studio configuration utilizing an HD camera, and the other half were generated through the application of image data augmentation methods. The Brix measurements were obtained using a Brix refractometer. The aforementioned values were subsequently employed to allocate categorical designations to the visual representations. The dataset is composed of a total of 300 data points, consisting of 150 unaltered images, 150 images that have been subjected to augmentation, and 300 Brix labels that correspond to the respective images. The algorithm initiates the process by extracting image features through the utilization of the ResNet101 architecture, which is a profound learning model that is renowned for its exceptional feature extraction capabilities.

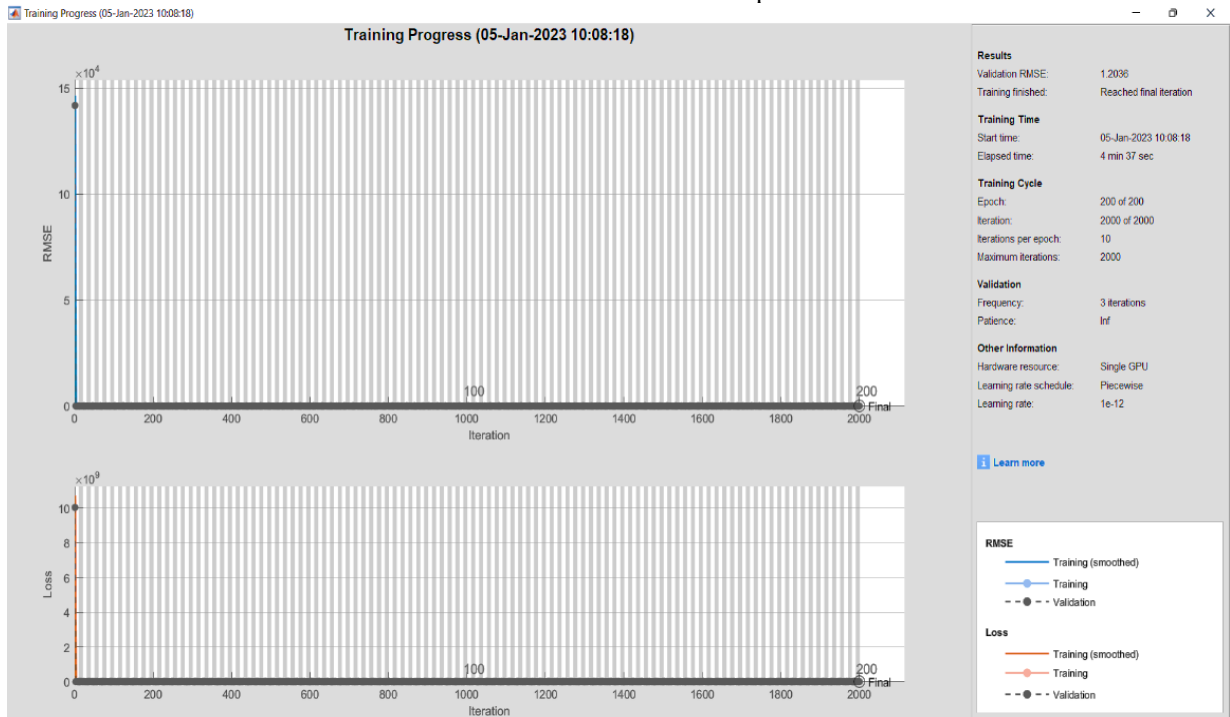


Fig. 14 Custom DL CNN-Based-Regression-Training Progress Plot

Table 6. Regression Progress Data using a Custom DL Regression Model.

No: of Samples	No: of Epochs	Iterations Per Epoch	Max Iterations	Elapsed Time	Validation RMSE
150 Images	200	10	2000	4 min 37 sec	1.2036

These image features are employed as input to the machine learning model in the course of its training procedure. The dataset has been segregated into two discrete subsets, namely a training set that constitutes 70% of the data and a testing set that constitutes the remaining 30%. After the training process, the best-trained model was exported and utilized to predict the Brix values of test samples. The algorithm presented in this research has exhibited a significant degree of predictive exactness, achieving a 96.3142% accuracy rate by employing the exponential model of Gaussian Process Regression (GPR). This observation denotes the algorithm's proficiency in precisely forecasting Brix values in strawberries by utilizing their image characteristics. Upon comparison with prior research, this study exhibits several unique and original characteristics. Incorporating a composite dataset that includes both original and augmented images amplifies the training data's variety and resilience. This methodology takes into consideration the diversities in the physical attributes of strawberries and furnishes the algorithm with an all-encompassing comprehension of the diverse visual traits of strawberries.

Furthermore, incorporating machine learning and deep learning methodologies enables the algorithm to harness the capabilities of both techniques. Utilizing the ResNet101

model for feature extraction facilitates the capture of high-level representations of strawberry images, thereby enhancing the precision of predictions. Moreover, the attained level of predictive precision highlights the algorithm's exceptional efficacy in forecasting Brix values in contrast to pre-existing techniques. The demonstrated level of precision showcases the effectiveness and dependability of the suggested methodology in evaluating the quality of strawberries through visual data.

Numerous investigations using vis/NIR techniques have been carried out globally over the past few years to estimate the Brix values of various fruits and vegetables [41-44,49]. Nondestructive NIR spectroscopy appears to be a viable technique for fruit quality assessment; however, it requires complex and expensive technology. The spectroscopic technique still has several limitations, even though it is thought to be the most practical way for non-destructive quality analysis of fruits and vegetables. The method's primary drawback is that it relies on reference values that could contain mistakes. For each fruit species, a fresh calibration model is necessary. It is preferable to enhance calibration models in accordance with variations in location and seasonal conditions.

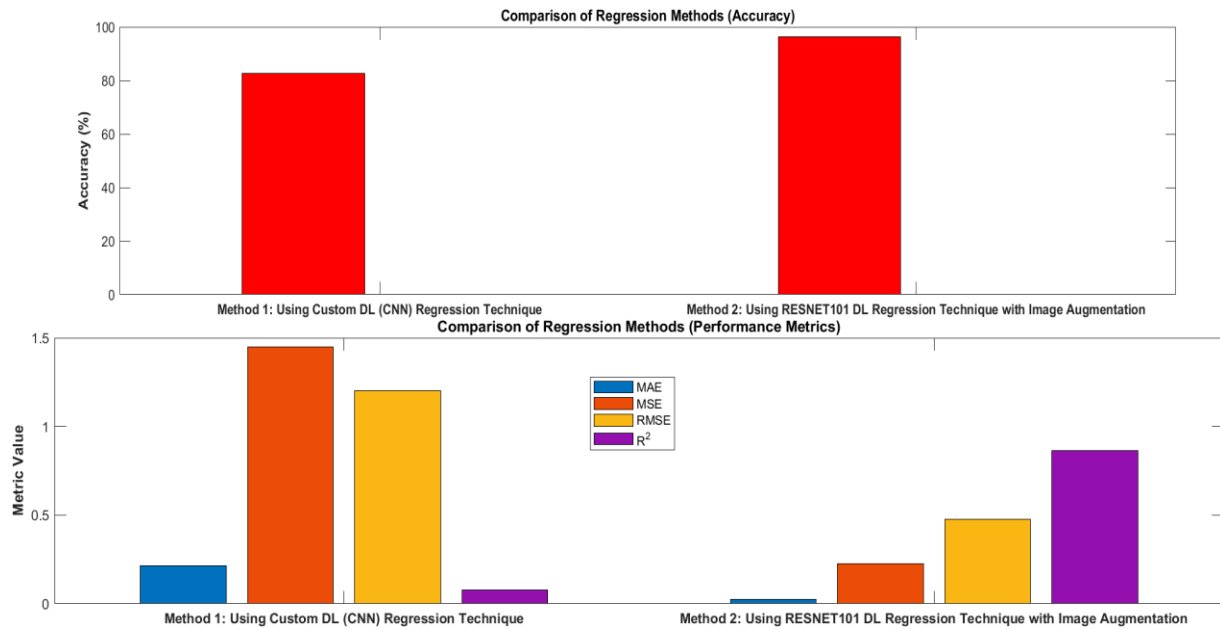


Fig. 15 Performance Metrics Comparison of both the methods (Method 1: A Custom DL- Based-Regression Technique, Method 2: Regression Technique using a Pre-Trained Model (ResNet101) and Image Augmentation Technique

Although there are many different techniques and tools for measuring Brix, the industry continues to place a high priority on attributes, including rapidity, affordability, little sample preparation, and environmental responsibility. As a result, a real-time, quick, non-invasive, and ongoing monitoring strategy for sugar value prediction is constantly needed. The proposed method can attain all these traits for

predicting Brix values by utilizing an automated function with the help of artificial intelligence. Many works in literature use machine learning techniques to classify fruits based on maturity. However, work related to the prediction of the Brix values of strawberries using regression-based deep learning techniques is very few. In those, the performance accuracy of prediction of the sugar value prediction is also not mentioned.

In the year 2020, Mancini and peers published a paper that presents a method for predicting the quality attributes of strawberries. [45] This study evaluated five strawberry genotypes using typical lab methods and non-destructive Near Infrared Spectroscopy (NIR). Principal Component Analysis (PCA) was used to discover spectral differences across samples, while partial least square (PLS) regression was used to predict quality metrics. PLS predicted soluble solids concentration and hardness well, making it appropriate for quality control. Soluble solids and Brix are two units of measurement for the concentration of soluble solids in a liquid, such as sugars. They are frequently used interchangeably to describe the sweetness degree of fruit juices. [46] In infrared, NIR spectroscopy helped assess strawberry fruits' chemical and physical qualities without destroying them. The study showed that PCA can estimate genotype spectral similarity, and Fourier Transform-NIR with PLS can predict qualitative parameters. An external test set confirmed that this algorithm using PLS regression for predicting soluble solids content ($^{\circ}$ Brix) performed well among others. The model was constructed by employing nine latent variables following the spectra preprocessing using the first derivative technique, specifically the Savitzky-Golay method, with a window size of 21 points and a second-order polynomial. The following performance measures were obtained for the prediction model, an RMSEP value of 0.8, a coefficient of determination value of 0.82, and an RPD value of 1.04. However, it was suggested that more research is needed for color and titratable acidity prediction as they did not give a satisfactory performance result.

When comparing the proposed system to the approaches outlined in [45], the proposed approach is simple and transparent in the techniques used for Brix prediction. The Brix values are predicted from strawberry images in a much simpler way using the pre-trained deep learning network, ResNet101, and to enhance the dataset size, a visual enhancement technique was employed in conjunction with feature extraction that helps in improved model generalization for an ML-based regression technique. According to the findings, the Squared Exponential GPR model, in conjunction with the enhanced dataset, was highly effective in forecasting the Brix scores of the test data samples. During the Brix prediction phase of the test data samples, the best model had a minimum RMSE of 0.4772. Furthermore, throughout the testing phase, the model was able to explain up to 86.48% of the variation in Brix measurement and prediction data of the test data samples. A model with a high R-squared value and a low RMSE value is generally considered highly effective and reliable. This Brix prediction system's overall forecasting precision was calculated to be 96.3142%. Using only strawberry images and Brix labels, the squared Exponential Gaussian Process regression model could effectively predict Brix values by incorporating a pre-trained deep learning-based method for image feature extraction and image data augmentation approaches. This accurate and dependable

method can be used to evaluate strawberry quality based on sweetness. The automation involved in the Brix value prediction using only images of strawberries makes this implementation method remarkable, which is made possible by training a regression algorithm to recognize patterns in the images and their corresponding Brix values. Also, this proposed approach requires strawberry juice extraction to assess the Brix values only during the training phase. Once the regression model has been built by training and testing with enough data samples, thereby achieving a 100% efficient model, strawberry destruction will no longer be needed to predict Brix values. More training data samples can be considered to achieve 100% performance accuracy. Table 6 demonstrates a comparison of the performance measures of the Brix prediction algorithm in literature [45] with the proposed method. The proposed method displays an R-squared and RPD value better than that of the best model in [45], which uses the PLSR technique, and also a lesser RMSEP value.

In a work published by Hayato Seki et al., an innovative method for assessing sugar levels in white strawberries through the utilization of near-infrared hyperspectral imaging (NIR-HSI) was introduced. [47] This novel preprocessing technique was developed to autonomously separate the flesh and achene on the surface of the fruit by integrating principal component analysis (PCA) and image processing. The predictive accuracy of the Partial Least Squares Regression (PLSR) model, which was constructed using the unprocessed spectra acquired from the flesh Region of Interest (ROI), was found to be satisfactory. This conclusion is supported by the Root Mean Square Error of Prediction (RMSEP) value of 0.576 and the R-squared value of 0.841. Additionally, the model was constructed using a relatively small number of PLS factors. The model exhibited a satisfactory level of predictive accuracy. The Brix heat map images and violin plots were employed to visually represent the characteristics of the sugar level distribution within the flesh of white strawberries.

A bar chart displayed in Figure 16 gives a comparison between the performance of the internal quality parameters prediction algorithms in literature [45], [47] with that of the proposed system. Here the performance metrics of the proposed method are compared with the best performance metric value obtained in [45] and [47] for the prediction of internal quality parameters in terms of R^2 and RMSEP values. When conducting a comparison of various regression models, it is typically preferable to observe a higher value for the coefficient of determination (R-squared) and a lower value for the root mean square error (RMSEP). A larger R-squared value signifies that the model accounts for a greater proportion of the variability in the dependent variable, implying a more optimal fit. A lower root mean square error (RMSEP) signifies that the model's predictions exhibit a higher degree of proximity to the observed values, thereby indicating enhanced accuracy.

An automated prediction system for strawberry harvesting time, sugar content, and acidity using image processing was proposed by Wanhyun Cho et al. in 2019 [48]. This work was accomplished in three different phases; initially, the researchers examined a segmentation method based on the ellipsoid Hough transform. This method aimed to segment the actual strawberry image automatically. Subsequently, the utilization of HSV color representations along with histogram-based color features was explored to differentiate between the three phases of strawberry development. The classification accuracy achieved for this task was 87.25%.

Moreover third, they investigated the partial least square regression (PLS model), a statistical analytic method for predicting strawberries' sugar concentration and acidity based on ripeness phases. The Brix prediction accuracy was not mentioned as such. The efficacy of the proposed prediction system was evaluated by conducting tests using diverse strawberry measurement data obtained from Gangwon-do

Highland in Korea. It is said that according to the experimental results, this prediction system could reasonably predict the sugar content and acidity of only the immature (White or Turning red phases) strawberries. However, the algorithm was unable to forecast the sugar level or acidity of the mature-ripe strawberries precisely. The model's predictive ability was deemed inadequate due to the imperfections present in the real data sets.

To summarize, the research presented in this study proposes a new algorithm that utilizes ML and DL-based image features to predict Brix values in strawberries. This algorithm is distinguished from prior research due to its utilization of an augmented dataset, implementation of feature extraction utilizing ResNet101, and notable predictive accuracy of 96.3142%. The present study makes a significant contribution towards the progression of the domain of strawberry quality evaluation. It exhibits potential for utilization in fruit quality management and enhancement in the agricultural sector.

Table 7. Comparison of performance measures of prediction algorithms for internal quality parameters (Soluble Solids/Brix) in literature [45], with

Comparison	Model Name	Dataset (Prediction Phase)	R ²	RMSEP	RPD
Method In Literature [45]	PLSR	9 latent variables after pre-treating the spectra with the first derivative (Savitzky–Golay method, 21 points window, second-order polynomial)	0.82	0.8	1.04
Proposed Method	Squared Exponential GPR	Augmented Dataset and Image Features (1000) Extracted using ResNet101 Pre-trained CNN model	0.8648	0.4772	2.7

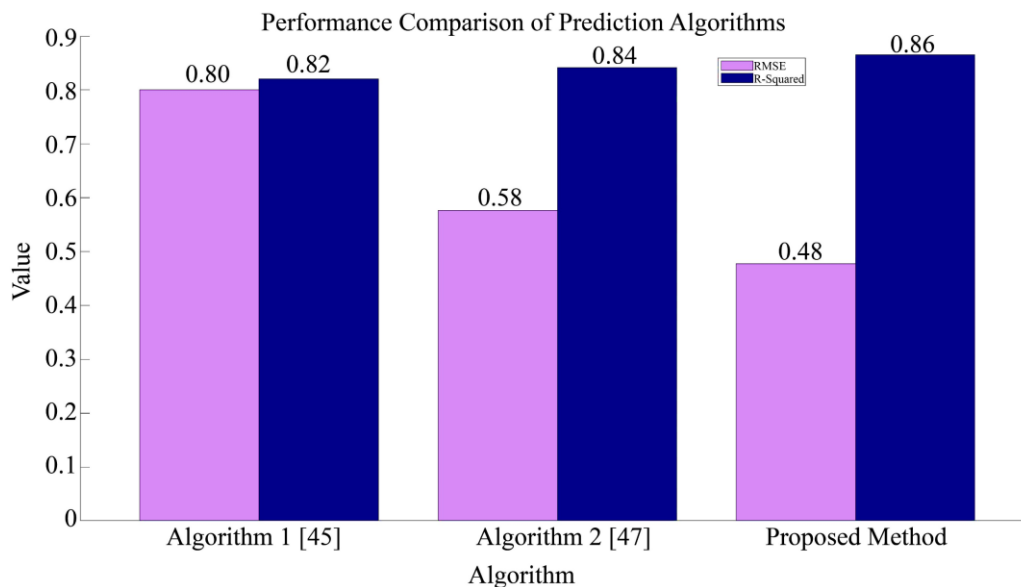


Fig. 16 Performance comparison bar plot of prediction algorithms in literature [45], [47] with the proposed method in terms of RMSEP and R² values. the proposed method

6. Conclusion

The precise estimation of Brix values in strawberries holds significant importance in evaluating their quality and managing them post-harvest. Regression techniques in deep learning have demonstrated potential in effectively capturing intricate patterns and extracting significant features from images. This work compiled a dataset of strawberry images and their corresponding Brix values of 150 strawberry samples by acquiring the image dataset and Brix values. Using the dataset, two distinct methodologies were employed to predict the Brix values of strawberries. The initial approach employed the utilization of obtained images and corresponding Brix values for the purpose of training a customized deep-learning regression model (Method 1).

The model could predict the Brix values of the test data samples, albeit with a moderate level of precision. The second approach (Method 2) utilized an image data augmentation methodology to augment the dataset along with a deep learning model for image feature extraction. Subsequently, it utilized a machine learning algorithm to predict Brix values with a high degree of precision. This was accomplished by training the algorithm with image features that were extracted through the utilization of a pre-trained deep learning method, specifically, ResNet 101. The extracted and normalized image features, as well as the corresponding Brix values, were trained using several regression methods so that they could learn the relation between the features of the image and their associated Brix values. After training, the best model with the minimum RMSE value, which is the GPR Squared Exponential model, was exported to the workspace and was able to predict the Brix values of the remaining test data samples from their images with high-performance measures.

The algorithm was able to achieve a prediction accuracy of 96.3142% with an RMSEP value of 0.4772, an MSE of 0.2277, an MAE of 0.0233, an RPD of 2.7, and a MAPE of 3.6858 after prediction. The model demonstrated the ability to account for a maximum of 86.48% of the variance in the predicted Brix values by utilizing the image feature variables of the previously unseen data. Agricultural practitioners and strawberry exporters can employ the suggested methodology to establish a commercially viable setup capable of automatically detecting the sweetness level of strawberries with a 100% precision rate. This can be achieved by training the system with a sufficient number of samples. The selection of the methodology ought to take into account the particular demands of the application, the resources that are at hand, and the desired levels of precision. Although Method 2 exhibited

superior accuracy compared to Method 1, it necessitates supplementary computational resources and a lengthier training period.

In contrast, Method 1 offers a relatively less complex approach but with a moderate level of precision. Subsequent investigations may concentrate on investigating alternative pre-trained deep learning models and refining augmentation methodologies to attain better precision in predicting Brix values for strawberries. Utilizing this methodology for the automated forecasting of Brix values in strawberries holds promise in improving the effectiveness of the network of supply chains by streamlining the delivery of fresh and high-quality strawberries to the market. As a result, this could lead to enhanced profitability and decreased wastage of produce. The implementation of this methodology has the potential to serve as a valuable instrument in enhancing the efficiency and accuracy of quality assurance protocols within the fruit sector, consequently augmenting the revenue and profitability of strawberry cultivators and merchants. In summary, the outcomes of this investigation demonstrate the capacity of image processing and artificial intelligence to influence the agricultural sector. Prospective implementations of this approach may encompass the automated and non-invasive forecasting of Brix levels in diverse types of berries and fruits.

Funding Statement

No funds, grants, or other support were received. On behalf of all authors, the corresponding author state that there is no conflict of interest.

Author Contributions

Ameetha Junaina T.K – Overall Design, Paper Writing, and Analysis.

R. Kumudham- Overall Co-ordination and Paper flow.

Ebenezer Abishek B- Analysis and Co-ordination.

Mohamed Shakir-Overall Co-ordination.

All authors approved the article for publication.

Acknowledgments

I am grateful for the valuable guidance provided by Dr. R. Kumudham, my research supervisor and Associate Professor at the Vels Institute of Science, Technology, and Advanced Studies. I also extend my appreciation to Dr. Ebenezer Abishek and Dr. Shakir Mohamed for their insightful comments on this work. Furthermore, I thank my family and friends for their constant encouragement and support throughout the process. Also, I would like to thank my university for the facilities provided.

References

- [1] Iqbal H. Sarker, "Deep Learning, A Comprehensive Overview on Techniques, Taxonomy, Applications, and Research Directions," *SN Computer Science*, vol. 2, p. 420, 2021. [[CrossRef](#)] [[Google Scholar](#)] [[Publisher Link](#)]
- [2] TechTarget, Website 2022. [Online]. Available: <https://www.techtarget.com/searchenterpriseai/definition/deep-learning-deep-neural-network/>

- [3] Mrs. T K Ameetha Junaina et al., "A Survey on Fresh Produce Grading Algorithms Using Machine Learning and Image Processing Techniques," *IOP Conference Series, Materials Science and Engineering*, vol. 981, 2020. [[CrossRef](#)] [[Google Scholar](#)] [[Publisher Link](#)]
- [4] Anjali Chandavale et al., "Automated Systems for Smart Agriculture," *IEEE Pune Section International Conference (PuneCon2019)*, pp. 1-6, 2019. [[CrossRef](#)] [[Google Scholar](#)] [[Publisher Link](#)]
- [5] Zeynep Ünal, "Smart Farming Becomes Even Smarter with Deep Learning—A Bibliographical Analysis", in *IEEE Access*, vol. 8, pp. 105587-105609, 2020. [[CrossRef](#)] [[Google Scholar](#)] [[Publisher Link](#)]
- [6] Kirtan Jha et al., "A Comprehensive Review on Automation in Agriculture Using Artificial Intelligence," *Artificial Intelligence in Agriculture*, vol. 2, pp. 1–12, 2019. [[CrossRef](#)] [[Google Scholar](#)] [[Publisher Link](#)]
- [7] M. Sowmiya, and S. Krishnaveni, "Deep Learning Techniques to Detect Crop Disease and Nutrient Deficiency - A Survey," *International Conference on System, Computation, Automation, and Networking*, pp. 1-5, 2021. [[CrossRef](#)] [[Google Scholar](#)] [[Publisher Link](#)]
- [8] Muhammad Hammad Saleem, Johan Potgieter, and Khalid Mahmood Arif, "Automation in Agriculture by Machine and Deep Learning Techniques: A Review of Recent Developments," *Precision Agriculture*, vol. 22, pp. 2053-2091, 2021. [[CrossRef](#)] [[Google Scholar](#)] [[Publisher Link](#)]
- [9] A. Subeesh, and C.R. Mehta, "Automation and Digitization of Agriculture using Artificial Intelligence and Internet of Things," *Artificial Intelligence in Agriculture*, vol. 5, pp. 278-291, 2021. [[CrossRef](#)] [[Google Scholar](#)] [[Publisher Link](#)]
- [10] Mohammad Amin Amani, and Francesco Marinello, "A Deep Learning-Based Model to Reduce Costs and Increase Productivity in the Case of Small Datasets: A Case Study in Cotton Cultivation," *Agriculture*, vol. 12, no.2, p. 267, 2022. [[CrossRef](#)] [[Google Scholar](#)] [[Publisher Link](#)]
- [11] Alberto Gutierrez-Torre et al., "Automatic Distributed Deep Learning Using Resource-Constrained Edge Devices," *IEEE Internet of Things Journal*, vol. 9, no. 16, pp. 15018-15029, 2022. [[CrossRef](#)] [[Google Scholar](#)] [[Publisher Link](#)]
- [12] Arteep Kumar et al., "Students' Academic Performance Prediction using Regression: A Case Study," *International Conference on System, Computation, Automation and Networking (ICSCAN)*, pp. 1-6, 2020. [[CrossRef](#)] [[Google Scholar](#)] [[Publisher Link](#)]
- [13] Redhat Website, 2022. [Online]. Available: <https://www.redhat.com/en/topics/automation/how-predictive-analytics-improve-it-performance/>
- [14] Xin Jia, "Image Recognition Method based on Deep Learning," *29th Chinese Control and Decision Conference (CCDC)*, pp. 4730-4735, 2017. [[CrossRef](#)] [[Google Scholar](#)] [[Publisher Link](#)]
- [15] Roberto Luciani, Giovanni Laneve, and Munzer JahJah, "Agricultural Monitoring, an Automatic Procedure for Crop Mapping and Yield Estimation: The Great Rift Valley of Kenya Case," *IEEE Journal of Selected Topics in Applied Earth Observations and Remote Sensing*, vol. 12, no. 7, pp. 2196-2208, 2019. [[CrossRef](#)] [[Google Scholar](#)] [[Publisher Link](#)]
- [16] Shubham Prabhu et al., "Soil Analysis and Crop Prediction," *International Journal of Scientific Research in Science and Technology*, pp. 117-123, 2020. [[CrossRef](#)] [[Google Scholar](#)] [[Publisher Link](#)]
- [17] Dhivya Elavarasan, and P. M. Durairaj Vincent, "Crop Yield Prediction Using Deep Reinforcement Learning Model for Sustainable Agrarian Applications," *IEEE Access*, vol. 8, pp. 86886-86901, 2020. [[CrossRef](#)] [[Google Scholar](#)] [[Publisher Link](#)]
- [18] Xiaojun Jin, Jun Che, and Yong Chen, "Weed Identification Using Deep Learning and Image Processing in Vegetable Plantation," *IEEE Access*, vol. 9, pp. 10940-10950, 2021. [[CrossRef](#)] [[Google Scholar](#)] [[Publisher Link](#)]
- [19] Lili Li, Shujuan Zhang, and Bin Wang, "Plant Disease Detection and Classification by Deep Learning—A Review," *IEEE Access*, vol. 9, pp. 56683-56698, 2021. [[CrossRef](#)] [[Google Scholar](#)] [[Publisher Link](#)]
- [20] Rupesh Gupta et al., "Automatic Identification of Paddy Crop Diseases using Deep Learning Approach," *3rd International Conference on Electronics and Sustainable Communication Systems*, pp. 915-920, 2022. [[CrossRef](#)] [[Google Scholar](#)] [[Publisher Link](#)]
- [21] Liu Liu et al., "Deep Learning Based Automatic Multiclass Wild Pest Monitoring Approach Using Hybrid Global and Local Activated Features," *IEEE Transactions on Industrial Informatics*, vol. 17, no. 11, pp. 7589-7598, 2021. [[CrossRef](#)] [[Google Scholar](#)] [[Publisher Link](#)]
- [22] Arnav Kumar et al., "Fruit-CNN: An Efficient Deep learning-based Fruit Classification and Quality Assessment for Precision Agriculture," *13th International Congress on Ultra Modern Telecommunications and Control Systems and Workshops (ICUMT)*, Brno, Czech Republic, pp. 60-65, 2021. [[CrossRef](#)] [[Google Scholar](#)] [[Publisher Link](#)]
- [23] Anuja Bhargava, and Atul Bansal, "Fruits and Vegetables Quality Evaluation using Computer Vision: A Review," *Journal of King Saud University - Computer and Information Sciences*, vol. 33, no. 3, pp. 243-257, 2021. [[CrossRef](#)] [[Google Scholar](#)] [[Publisher Link](#)]
- [24] Yanxiang Yang et al., "Deep Reinforcement Learning-Based Irrigation Scheduling," *Transactions of the ASABE*, vol. 63, no. 3, pp. 549-556, 2020. [[CrossRef](#)] [[Google Scholar](#)] [[Publisher Link](#)]
- [25] Khadijeh Alibabaei et al., "Irrigation Optimization with a Deep Reinforcement Learning Model: Case Study on a Site in Portugal," *Agricultural Water Management*, vol. 263, 2022. [[CrossRef](#)] [[Google Scholar](#)] [[Publisher Link](#)]
- [26] Pallavi V. Jirapure, and Prarthana A. Deshkar, "Qualitative Data Analysis using Regression Method for Agricultural Data," *World Conference on Futuristic Trends in Research and Innovation for Social Welfare (Startup Conclave)*, pp. 1-6, 2016. [[CrossRef](#)] [[Google Scholar](#)] [[Publisher Link](#)]

- [27] Veera Sellam, and Eswaran Poovammal, “Prediction of Crop Yield using Regression Analysis,” *Indian Journal of Science and Technology*, vol. 9, no. 38, 2016. [[CrossRef](#)] [[Google Scholar](#)] [[Publisher Link](#)]
- [28] Swapna A. Jaywant, Harshpreet Singh, and Khalid Mahmood Arif, “Sensors and Instruments for Brix Measurement: A Review,” *Sensor*, vol. 22, no. 6, p. 2260, 2022. [[CrossRef](#)] [[Google Scholar](#)] [[Publisher Link](#)]
- [29] Bowonsak Srisungsittisunti, “Forward Feature Selection for Ensembles to Predict Brix Values in Mango Fruits based on NIR Spectroscopy Technique,” *International Journal of Science*, vol. 15, no. 2, pp. 43-57, 2018. [[Google Scholar](#)] [[Publisher Link](#)]
- [30] Mustafa Ahmed Jalal Al-Sammarraie et al., “Predicting Fruit’s Sweetness Using Artificial Intelligence—Case Study: Orange,” *Applied Sciences*, vol. 12, no. 16, p. 8233, 2022. [[CrossRef](#)] [[Google Scholar](#)] [[Publisher Link](#)]
- [31] TK Ameetha Junaina et al., “Maturity Level Detection of Strawberries-A Deep Color Learning-Based Futuristic Approach,” *Futuristic Communication and Network Technologies*, Springer, Singapore, vol. 995, pp. 153-163, 2021. [[CrossRef](#)] [[Google Scholar](#)] [[Publisher Link](#)]
- [32] The Wikipedia Website, 2023. [Online]. Available: <https://en.wikipedia.org/wiki/Brix/>
- [33] Amazon Website, Brix Refractometer. [Online]. Available: <https://www.amazon.in/Refractometer-Hydrometer-Measuring-Saccharimeter-calibration/dp/B0B6DRM1DH/>
- [34] Matlab Website. [Online]. Available: <https://in.mathworks.com/help/matlab/ref/matlab.io.datastore.imagedatastore.html>
- [35] Matlab. [Online]. Available: <https://in.mathworks.com/help/deeplearning/ug/extract-image-features-using-pretrained-network.html>
- [36] Kaiming He et al., "Deep Residual Learning for Image Recognition," in *Proceedings of the IEEE Conference on Computer Vision and Pattern Recognition (CVPR)*, pp. 770-778, 2016. [[CrossRef](#)] [[Google Scholar](#)] [[Publisher Link](#)]
- [37] Matlab Website. [Online]. Available: <https://in.mathworks.com/help/deeplearning/ref/resnet101.html>
- [38] AnalyticsVidya Website. [Online]. Available: <https://www.analyticsvidhya.com/blog/2021/10/evaluation-metric-for-regression-models/>
- [39] Arzu Yazici, Gulgun Yildiz Tiryaki, and Huseyin Ayyaz, “Determination of Pesticide Residual Levels in Strawberry (*Fragaria*) by Near-Infrared Spectroscopy,” *Journal of the Science of Food and Agriculture*, vol. 100, no. 5, pp. 1980-1989, 2020. [[CrossRef](#)] [[Google Scholar](#)] [[Publisher Link](#)]
- [40] M. Amirthalingam, and R. Ponnusamy, "Intelligent Wireless Endoscopic Image Classification using Gannet Optimization with Deep Learning Model," *SSRG International Journal of Electrical and Electronics Engineering*, vol. 10, no. 3, pp. 104-113, 2023. [[CrossRef](#)] [[Publisher Link](#)]
- [41] Tanachart Sripaurya et al., “Gros Michel Banana Soluble Solids Content Evaluation and Maturity Classification using a Developed Portable 6 Channel NIR Device Measurement,” *Measurement*, vol. 173, p. 108615, 2021. [[CrossRef](#)] [[Google Scholar](#)] [[Publisher Link](#)]
- [42] Manuel Larrain, Andrés R. Guesalaga, and Eduardo Agosin, “A Multipurpose Portable Instrument for Determining Ripeness in Wine Grapes using NIR Spectroscopy,” *IEEE Transactions on Instrumentation and Measurement*, vol. 57, no. 2, pp. 294–302, 2008. [[CrossRef](#)] [[Google Scholar](#)] [[Publisher Link](#)]
- [43] Shyam N. Jha, and T. Matsuoka, “Non-Destructive Determination of Acid–Brix Ratio of Tomato Juice using Near-Infrared Spectroscopy,” *International Journal of Food Science & Technology*, vol. 39, no. 4, pp. 425–430, 2004. [[CrossRef](#)] [[Google Scholar](#)] [[Publisher Link](#)]
- [44] Kim Seng Chia et al., “Pre-Dispersive Near-Infrared Light Sensing in Non-Destructively Classifying the Brix of Intact Pineapples,” *Journal of Food Science and Technology* volume, vol. 57, pp. 4533–4540, 2020. [[CrossRef](#)] [[Google Scholar](#)] [[Publisher Link](#)]
- [45] Manuela Mancini et al., “Application of the Non-Destructive NIR Technique for the Evaluation of Strawberry Fruits Quality Parameters,” *Foods*, vol. 9, no. 4, p. 441, 2020. [[CrossRef](#)] [[Google Scholar](#)] [[Publisher Link](#)]
- [46] R. Dhiman, N. Garg, and M. Gupta, “Quality Characteristics of Strawberry Juice during Storage,” *Journal of Food Science and Technology*, vol. 50, no. 1, pp. 111–115, 2021.
- [47] Hayato Seki et al., “Visualization of Sugar Content Distribution of White Strawberry by Near-Infrared Hyperspectral Imaging,” *Foods*, vol. 12, no. 5, p. 931, 2023. [[CrossRef](#)] [[Google Scholar](#)] [[Publisher Link](#)]
- [48] Wanhyun Cho et al., “Automatic Prediction of Brix and Acidity in Stages of Ripeness of Strawberries Using Image Processing Techniques,” *34th International Technical Conference on Circuits/Systems, Computers, and Communications (ITC-CSCC)*, pp. 1-4, 2019. [[CrossRef](#)] [[Google Scholar](#)] [[Publisher Link](#)]
- [49] Rasool Khodabakhshian et al., “A Comparative Study of Reflectance and Transmittance Modes of Vis/NIR Spectroscopy Used in Determining Internal Quality Attributes in Pomegranate Fruits,” *Journal of Food Measurement and Characterization*, vol. 13, pp. 3130–3139, 2019. [[CrossRef](#)] [[Google Scholar](#)] [[Publisher Link](#)]